EFDA–JET–CP(09)06/33

E.R. Solano, P.J. Lomas, B. Alper, G. Xu, Y. Andrew, G. Arnoux, A. Boboc, L. Barrera, P. Belo, M.N.A. Beurskens, M. Brix, K. Crombe, E. de la Luna, S. Devaux, T. Eich, S. Gerasimov, C. Giroud, D. Harting, D. Howell, A. Huber, G. Kocsis, A. Korotkov, A. Lopez-Fraguas, M.F.F. Nave, C. Pérez Von Thun, E. Rachlew, F. Rimini, S. Saarelma, A. Sirinelli, L. Zabeo, D. Zarzoso and JET EFDA contributors

# High Temperature Pedestals in JET and Confined Current Filaments

# High Temperature Pedestals in JET and Confined Current Filaments

E.R. Solano[1], P.J. Lomas[2], B. Alper[2], G. Xu[3], Y. Andrew[2], G. Arnoux[2], A. Boboc[2], L. Barrera[1], P. Belo[4], M.N.A. Beurskens[2], M. Brix[2], K. Crombe[5], E. de la Luna[1], S. Devaux[6], T. Eich[6], S. Gerasimov[2], C. Giroud[2], D. Harting[7], D. Howell[2], A. Huber[7], G. Kocsis[8], A. Korotkov[2], A. Lopez-Fraguas[1], M. F. F. Nave[4], C. Pérez Von Thun[6], E. Rachlew[9], F. Rimini[10], S. Saarelma[2], A. Sirinelli[2], L. Zabeo[2], D. Zarzoso[11] and JET EFDA contributors*

***JET-EFDA, Culham Science Centre, OX14 3DB, Abingdon, UK***

*[1]Laboratorio Nacional de Fusión, Asociación EURATOM-CIEMAT, 28040, Madrid, Spain*
*[2]EURATOM/UKAEA Fusion Association, Culham Science Centre, Abingdon, Oxon, OX14 3DB, UK*
*[3]Institute of Plasma Physics, Chinese Academy of Sciences, Hefei 230031, China*
*[4]Associação EURATOM/IST, Inst. de Plasmas e Fusão Nuclear, Av Rovisco Pais, 1049-001, Lisbon, Portugal*
*[5]Department of Applied Physics, Ghent University, Rozier 44, 9000 Gent, Belgium*
*[6]Max-Planck-Institut für Plasmaphysik, EURATOM-Assoziation, D-85748 Garching, Germany*
*[7]Forschungszentrum Jülich GmbH, Institut für Plasmaphysik, EURATOM-Assoziation, TEC, D-52425 Jülich, Germany*
*[8]KFKI, Association EURATOM, P.O.Box 49, H-1525, Budapest, Hungary*
*[9]Association EURATOM-VR, Department of Physics, SCI, KTH, SE-10691 Stockholm, Sweden*
*[10]EFDA Close Support Unit, Culham Science Centre, Culham, OX14 3DB, UK*
*[11]Ecole Polytechnique, F-91128, Palaiseau Cedex, France*
** See annex of F. Romanelli et al, "Overview of JET Results",*
*(Proc. 22 [nd] IAEA Fusion Energy Conference, Geneva, Switzerland (2008)).*

Preprint of Paper to be submitted for publication in Proceedings of the
36th EPS Conference on Plasma Physics, Sofia, Bulgaria.
(29th June 2009 - 3rd July 2009)

## 1. INTRODUCTION

High temperature pedestals can be obtained in JET, transiently, by reducing recycling and operating at initially low density in the hot ion H-mode regime [1]. The L-H transition occurs at low density, and after the transition the pedestal density, rotation and temperatures rise up until the occurrence of the first natural ELM. Recent examples at JET reach $T_{e,ped}$ = 2.8keV before the 1st ELM. Often the obstacle to reaching higher pedestal temperatures is MHD. Here we report on MHD observations in hot ion H-modes in high triangularity plasmas with 2.5MA, 2.7T and 15MW of Neutral Beam Injection heating.

During the ELM-free period of hot-ion H-mode plasmas MHD instabilities known as Outer Modes (OM) in JET are sometimes observed [2,3]. Time traces of an especially long OM are shown in Fig.1: $D_\alpha$, electron density ne, electron and ion temperature ($T_e$ and $T_i$) and toroidal rotation frequency ($f_{tor}$). The profile quantities are taken at R = 3.78m, the top of the pedestal, inboard of the pedestal knee. Also shown is the spectrum (FFT) of a Mirnov coil. At the L to H transition, in this case marked by the initial $D_\alpha$ drop, pedestal values rise as usual. At the time t,= 13.98s, $D_\alpha$ rises, while the pedestal Te begins to drop and the toroidal rotation frequency remains fairly constant. Density continues to rise, albeit slower than before. At the end of the OM the pedestal density has risen from $3.7\times10^{19}$ $m^{-3}$ to $4.5\times10^{19}$ $m^{-3}$. The $D_\alpha$ drop signals the end of the very high confinement phase of the ELM-free period, coinciding with the appearance of the OM. The H factor drops down from a maximum value of $H_{98}$ = 1.4 to a steady value of $H_{98}$ = 1.1 at the outset of the OM. A comparison of the profiles of rotation, density and temperatures is shown in Fig. 2. After the first ELM the pedestal density rises to $5.6\times10^{19}$ $m^{-3}$ due to impurity penetration [4] and thereafter ne,core rises slowly during the ELMy phase. In this particular pulse the OM survives 2 sawtooth crashes, indicating that it is a robust feature of the plasma. There is a brief quiet interval between the end of the OM at 15.375s and the ELM at 15.430s, indicating that the OM is not an ELM precursor, but a different instability. In this particular pulse the OM does not return after the first ELM. In other pulses it sometimes returns with ever decreasing duration some hundreds of ms after the first few ELMs. The OM often appears when recycling and fuelling are particularly low, and it can be reduced or eliminated by increased fuelling. The ELM-free period is prolonged by the presence of the OM: a pulse with the same conditions but more fuelling ($1.9\times10^{21}$ instead of $1.5\times10^{21}$ e/s, note both values are very low) had no long-lived OMs and the first ELM occurred 1s sooner, at 14.4s.

The most clear signature of the OM is in the FFT of the Mirnov signals: its harmonic structure, shown in Fig.1(e). The fundamental harmonic has frequency f = 6kHz and toroidal mode number n = 1, and every subsequent harmonic has n increased by 1. Typically harmonics are seen up to 45kHz (n = 7), but the mode is sometimes clearly recognisable up to 90kHz (n = 15). This rich harmonic structure is a clear indicator of strong localisation of the current source that produces the magnetic fluctuation. But the raw magnetic signals contain more information than their spectrum. Plotted in Fig.3 are signals from a toroidal array of Mirnov coils, measuring the vertical field at

different toroidal angles around the device. Plotted at the bottom of the same figure is an integrated signal: discrete blips can be clearly seen, propagating toroidally with f = 6kHz, due to a localised current structure. The sign of the blips indicate that this co-rotating current structure carries excess current relative to the axisymmetric equilibrium current profile. Since the current feature is long-lived, it must be located inside the separatrix, and must be aligned with the magnetic field at a rational surface. Analysis of the magnetic signals show that the current structure is best simulated as a current ribbon with excess current of 100-200 A, with n = 1, m = 4, rotating toroidally at 6kHz, as illustrated in Fig.4. Data in 1 inboard coil is substantially better fitted by q = 4 than by q = 2, but none of the other coils can distinguish these two cases.

The spectra of various fluctuation measurements show multiple harmonics of the mode near the gradient region. Interferometry indicates that the mode is strongest at the iso-density layer with $n_e = 2.5\times10^{19}$ $m^{-3}$ early on. Towards the end of the OM the pedestal density has risen and the mode becomes visible at $n_e = 5.\times10^{19}$ $m^{-3}$, inboard of the density pedestal. Fluctuations of $D_\alpha$, Electron Cyclotron Emission in the $T_e$ gradient region and edge channels of Soft X-Rays, all show at least 3 harmonics of the OM. Fluctuations of $n_e$ and $T_e$ are localised by $|B|$ and are particularly sensitive to gradients: it is not possible to establish from these measurements if the current ribbon is located at the top of the pedestal, where their sensitivity is much reduced. Data from high field side ECE channels show that the OM is not a tearing mode [5].

Characteristic profiles at the onset and at the end of the OM were shown in Fig.2(a) and 2(b). From the charge-exchange measurements of the toroidal ion rotation frequency and in the usual assumption that the fluid velocity is dominated by the ion velocity, we can identify the radial position of the current ribbon. Early in the OM it appears that the location of the mode is as the top of the density pedestal, at the edge of the ion rotation gradient region, inboard of the maximum pressure gradient. At the end of the OM the toroidal rotation shear is greatly eroded and the mode is located in the toroidal rotation gradient region, albeit still inboard of the density and temperature high gradient regions.

The heat flux to the outer divertor target was measured with a fast Infra-Red (IR) camera, with a frame rate especially set to 1/38ms, and an integration time of 27ms. Soon after the mode sets in, the average heat flux to divertor rises from 10-15MW/$m^2$ to 25-30MW/$m^2$. Periodically (1/6kHz), bursts of heat arrive away from the maximum deposition location, as shown in Fig.5. Both, strong overall transport, and a time-localised “hose-pipe” contribute to heat flux on to target during the OM. This is most easily explained by a mixture of partial ergodisation and homoclinic tangles [6]. A rotating even mode at the top of the pedestal produces partial ergodisation of field lines in the pedestal region, increasing overall heat flux. At a specific toroidal location a particular flux tube can escape through the broken X-point and deliver intermittent heat flux away from the main strike position.

A linearized ideal MHD analysis (Mishka-1 [7]) of the plasma before and during the OM shows no evidence of instability to n = 1. Earlier understanding of the OM as an external kink [3] may need to be revisited. A vortex solution of ideal MHD is a non-linear effect driven by  and it is

unlikely to be picked up by linear codes. We speculate that either the high Te,ped and/or the high rotation velocities present in the plasma before the mode onset leads to the circumstances necessary for current filaments (MHD vortices) to form and survive.

Note that the OM is very similar to the Edge Harmonic Oscillation of Quiescent H-modes of DIII-D and AUG, as described in [8,9]. Further studies of this phenomenon in JET may enable us to design OMs and QH phases for ITER operation.

## REFERENCES


[1]. JET Team, presented by P.J. Lomas, Plas. Phys. & Contr. Nucl. Fus. Res. 1994 (Proc. 15th Int. Conf. Seville, 1994), Vol. 1, IAEA, Vienna 211 (1995).

[2]. M.F.F. Nave *et al*, Nuclear Fusion **35** 409 (1995)

[3]. G.T.A. Huysmans *et al*, Nuclear Fusion **38**, 179 (1998)

[4]. P. Belo, this conference, P2.165.

[5]. L. Barrera, this conference, P5.171.

[6]. T.E. Evans *et al*, J. Phys.: Conf. Ser. **7** 174 (2005)

[7]. A.B. Mikhailovskii *et al*, Plas. Phys. Rep. **23**, 844 (1997)


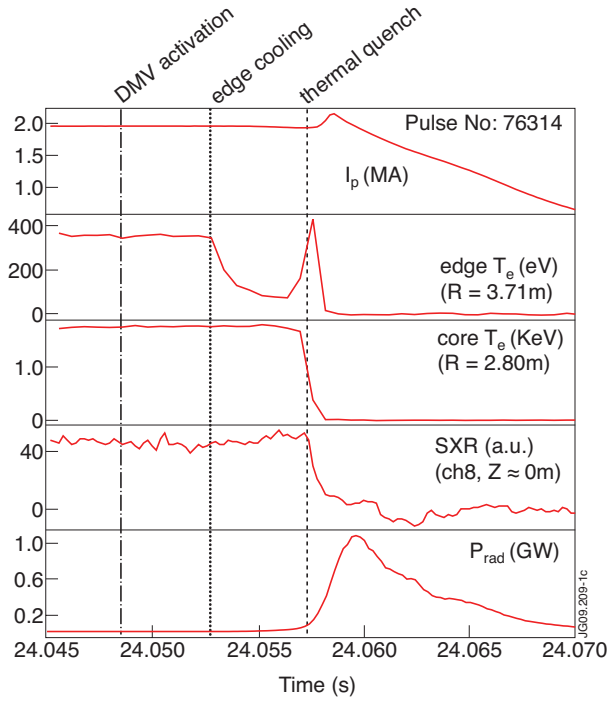


*Figure 1: time traces of a hot ion H-mode interrupted by an Outer mode, see text.*

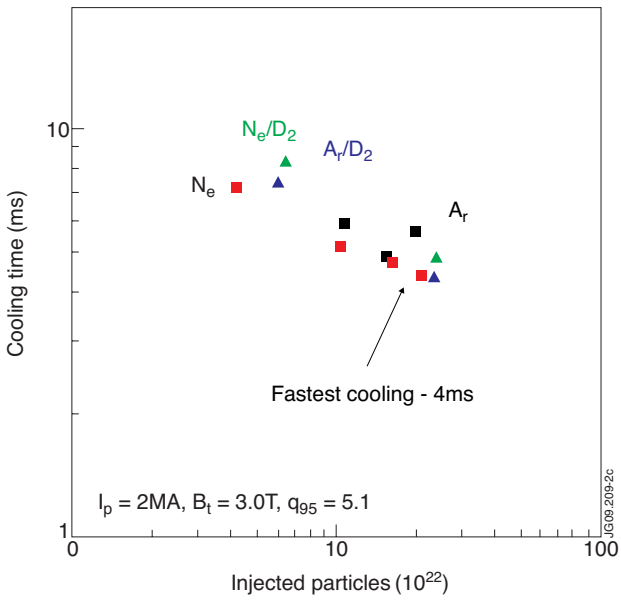


*Figure 2: profiles of toroidal rotation frequency, $n_e$, $T_e$, $T_i$ start (top) and end of OM.*

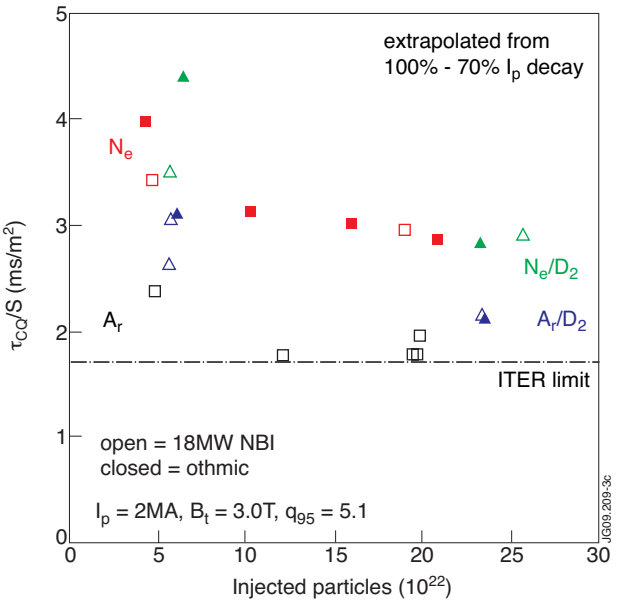


*Figure 3: (left): Mirnov coil signals from toroidal array, showing toroidal propagation of current feature in co-current direction. The lowest plot is the integrated signal from coil at 3º.*

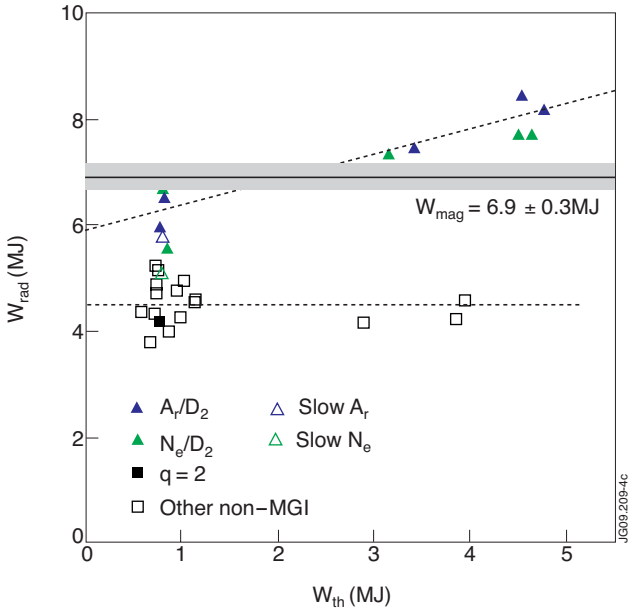


*Figure 4: q=4 current ribbon that provides best fit to magnetic signals from Mirnov coil set, with current 100-200A.*

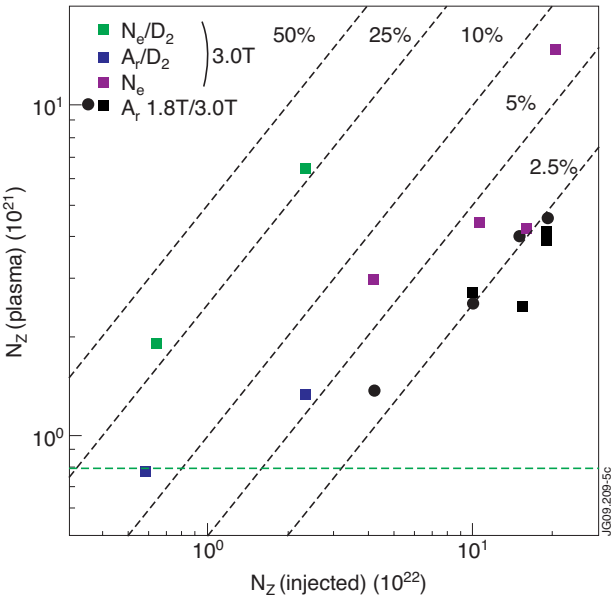


*Figure 5: heat flux contours at outer strike are, measured with IR, and integrated magnetic signal showing synchronisation of heat pulses with OM.*